The Laschamp geomagnetic field excursion recorded in Icelandic lavas

A. Ferk, R. Leonhardt

▶ To cite this version:

A. Ferk, R. Leonhardt. The Laschamp geomagnetic field excursion recorded in Icelandic lavas. Physics of the Earth and Planetary Interiors, 2009, 177 (1-2), pp.19. 10.1016/j.pepi.2009.07.011 . hal-00585469

Accepted Manuscript

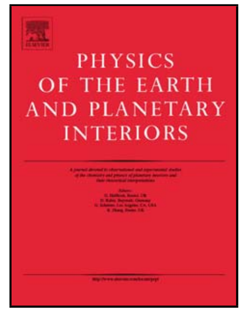

Title: The Laschamp geomagnetic field excursion recorded in Icelandic lavas

Authors: A. Ferk, R. Leonhardt

PII: S0031-9201(09)00147-2
DOI: doi:10.1016/j.pepi.2009.07.011
Reference: PEPI 5179

To appear in: *Physics of the Earth and Planetary Interiors*

Received date: 25-11-2008
Revised date: 5-6-2009
Accepted date: 1-7-2009

Please cite this article as: Ferk, A., Leonhardt, R., The Laschamp geomagnetic field excursion recorded in Icelandic lavas, *Physics of the Earth and Planetary Interiors* (2008), doi:10.1016/j.pepi.2009.07.011

The Laschamp geomagnetic field excursion recorded in Icelandic lavas

A. Ferk [a,b], R. Leonhardt [a]

[a] *Department of Applied Earth Sciences and Geophysics, Montanuniversity, 8700 Leoben, Austria*

[b] *Department of Earth and Environmental Sciences, Ludwig-Maximilians-University, 80333 Munich, Germany*

Abstract

We sampled 28 lava flows and a tephra layer, dated at about 40 kyr, at the Reykjanes Peninsula, Iceland. 10 flows and the tephra recorded what has been originally referred to as the Skalamælifell geomagnetic field excursion. The age of this excursion (42.9±7.8 ka) is statistically indistinguishable from the Laschamp excursion (40.4±2.0 ka). Rock magnetic investigations show that the main remanence carriers are (titano-) magnetites with different degrees of oxidation. One excursional flow exhibits partial self-reversal behavior; however, it could be shown by continuous thermal demagnetization that its paleodirection is unaffected. We subjected 52 samples from 16 flows to Thellier-type paleointensity determinations. Reliable paleointensity data were obtained for 10 of the 29 sites. In the beginning of the excursion virtual geomagnetic poles (VGPs) in the Southeast Pacific are recorded. These sites are characterized by paleointensities of 4 to 5 μT, about 1/10 of the intensity of the normal polarity flows, which ranges from 27.4 μT to 59.3 μT. Towards the end of the excursion, VGPs are found in North Africa. At these sites paleointensity has already regained about half of its original value (19.9±2.4 μT).

Preprint submitted to Elsevier Science *5 June 2009*

A comparison of the paleointensity data with the results of previous studies gives a very consistent picture, as all records show almost identical intensity values during the Skalamælifell excursion. A tentative stratigraphic relationship between 25 sites prior to, during and after the Skalamælifell excursion was established by comparing them with virtual geomagnetic poles (VGPs) from different marine sedimentary records. Only VGPs from four flows could not be matched unambiguously to those of the marine records. Our results support the theory that the geomagnetic field during the Laschamp excursion likely had a simple transitional field geometry at least during the onset of the excursion. The data are best explained by a decrease of the axial dipole field and a substantial transitional equatorial dipole field that was accompanied by a considerably reduced non-dipole field.

Key words: Geomagnetism, Palaeomagnetism, Excursion, Laschamp, Iceland

1 Introduction

The actual normal polarity chron (Brunhes) has lasted already 0.78 Myr, which is much longer than the average duration of any other polarity epoch during the last 5 Ma. In this interval, however, several global geomagnetic field excursions like Big Lost (0.6 Ma) and the Emperor (0.5 Ma) are present (e.g. Laj and Channel, 2007). Excursions are defined as short-duration directional changes, which exceed normal secular variation. They may either denote anomalous high secular variation or reflect an aborted reversal (Lund et al., 2006; Valet et al., 2008). Further excursions have been reported for the last 0.1 Ma, e.g. the Mono Lake excursion (≈32,4 ka) (Benson et al., 2003) and the Laschamp excursion (≈40 ka) (Bonhommet and Babkine, 1967). A detailed

Email address: `ferk@geophysik.uni-muenchen.de` (A. Ferk).

paleomagnetic investigation is essential to enlarge our knowledge of the geomagnetic field generation during such disturbances. It has been suggested that the Earth's inner core is responsible for the difference between excursions and reversals (Gubbins, 1999). One possible process could be that during excursions the field reverses only in the outer core (overturn time 500 years) and then switches back. During reversals (timescales of about 3000 years) the inner core field reverses as well. Comparing paleomagnetic results from different global locations could shed light on the global morphology of the geomagnetic field during such disturbances (Leonhardt et al., 2009). The majority of excursions have so far been recorded in sediments. However, 40 years ago Bonhommet and Babkine (1967) found evidence for an excursion in Quaternary lava flows of the French Massif Central: The Laschamp event. It was later estimated to have occurred about 40 ka ago (Guillou et al., 2004). The same excursion was reported in marine sediments at e.g. Bermuda Rise and Blake Outer Ridge (Lund et al., 2005), the Gulf of California (Levi and Karlin, 1989) and in the North Atlantic (Channell, 2006). In 1980, Kristjánsson and Gudmundsson (1980) observed an excursion, the Skalamælifell excursion, in three hills on the Reykjanes Peninsula, Iceland. At 95% confidence level this excursions age (42.9±7.8 ka) (Levi et al., 1990) is indistinguishable from the one of the Laschamp excursion (40.4±2.0 ka) (Guillou et al., 2004). Age determinations were done by Levi et al. (1990) on 19 icelandic samples of which 6 are from sites that correspond to our sites at Bleikshóll. Levi et al. (1990), as well as Kristjánsson (2003), also performed further field work, and some studies were done on paleointensities (Levi et al., 1990; Marshall et al., 1988), showing that throughout the excursion the intensity was just about 1/10 of the intensity of normal polarity sites. As some of the former studies at Skalamælifell were mainly designed to look for excursional lava flows, just one or two samples were taken at each site and often the specimens were not fully demagnetized, but retained still 90 to 95% of the natural remanent magnetization (NRM), when the paleodirections were determined. A further aspect is that so far, no stratigraphy could be established as the sampled volcanic structures are isolated and their products do seldom overlap. Examining different marine sedimentary records of the Laschamp excursion, Laj et al. (2006) found strikingly similar VGP paths with clockwise loops. They suggested that the simple structure of the paths indicates a simple geometry of the intermediate field and concluded that the field is dominated by a dipolar field. Thus, due to low intensities, both dipolar and non-dipolar fields must have been reduced. Recently obtained southern hemipshere paleomagnetic data for the Laschamp excursion is not consistent with such simple loops (Cassata et al., 2008) and a global field model of the Laschamp excursion, which utilizes the here presented data, also indicates a dominance of non-dipolar components for a brief time interval (Leonhardt et al., 2009). In order to either support or reject these differing ideas, further data on paleointensities and -directions are needed. In particular, accurate studies of igneous records are required to compare them to the results of the marine sediments.

For this study some of the volcanic structures in the area were sampled and measurements of paleodirection, rock magnetic parameters and paleointensity were carried out. For one sampled volcanic structure previous full vector paleomagnetic data existed, which could be confirmed by this study. Our results are compared with other excursion data of Laschamp and different sedimentary records, and combined in a stratigraphic correlation of the different sites. Finally, implications for the geomagnetic field are discussed.

2 Geological setting and sampling

Samples were taken on Reykjanes Peninsula in Southwest Iceland. The Reykjanes Peninsula, which is the onshore continuation of the Mid-Atlantic Ridge (Reykjanes Ridge), includes five volcanic systems/fissure swarms: Reykjanes, Grindavik, Krysuvik, Blafjoll and the easternmost Hengill system, which lies at a triple junction between Reykjanes Peninsula, Western Rift Zone and South Iceland Fracture zone. The Peninsula is an arid plain with a median altitude of 200 m in the east, 50 m in the west, and numerous volcanic structures that rise above the plain. Most of the lava flows and volcanic detritus are quite recent, but some of the volcanic structures erupted during the last glacial period. The products of the subglacial eruptions of these older hills are hyaloclastites, breccia and pillows as well as some lava flows (Levi et al., 1990). Some of these older volcanic structures were sampled in an area north-east of Grindavik. Fig. 1 shows a map of the sampling area (sampling locations are marked by abbreviations). As mentioned before, Kristjánsson and Gudmundsson (1980) detected shallow negative inclinations and westerly declinations on three different hills on Reykjanes Peninsula. Later, Levi et al. (1990) also found other flows with intermediate directions. For this study, suitable locations with excursional rocks were chosen by examining the work of Kristjánsson (2003) and Levi et al. (1990), and by oral communication with Kristjánsson in 2005. Altogether 181 samples were taken from 28 different lava flows and one tephra layer. Whenever possible six or more samples were taken at each flow and were oriented using both magnetic and sun compass, which were later found to show perfect accordance. For later comparison with previous works, it is important to mention, that Kristjánsson (2003) and Levi et al. (1990) used a different map, in which the hills are sometimes labeled differently. The Siglubergsháls on their map is north of the road, and thus, belongs to the area around Bleikshóll on the map used for this study. These sites were also sampled by Marshall et al. (1988). The only further overlap of our sampling area with those of previous full-vector studies is at Festarfjall and Siglubergsháls on our map, where Levi et al. (1990) took some samples as well. The other sites of Marshall et al. (1988) and Levi et al. (1990) lie east of our sampling area. Further, for future sampling in the area, it is important to note that some years ago a new road, north of the old one was built, which is not on the map. However, the old one is there still and orientation in the area should therefore be quite easy. The drilled flows consist mostly of grey, olivine rich basalts with many vesicles. Occasionally, feldspar phenocrysts are seen. The flows at Fagradalsfjall (FAG) are very thin, about 20 cm to 50 cm. Those at Nátthagakriki (N), Einbúi (E), Siglubergsháls (SI) and Festarfjall (FS) are about 1 to 2 m, sometimes even 3 m. At the base (B) we sampled the side wall of a lava tube. The roughly 50 cm thick tephra (TE) is baked in some parts, and has some lapilli layers inside. Identification of stratigraphic relationships between the different volcanic structures is very difficult as they are heterogeneous and isolated. Only the flank of Nátthagakriki and Fagradalsfjall are right next to each other. Field observation indicate that lavas from Fagradalsfjall overflowed onto part of the flank, suggesting that the flank is older than Fagradalsfjall. Our interpretation is that the base is the oldest section and that the various hills rose through it. For additional correlations, further information on paleodirections and paleointensities will be used later in this study. Whenever there was more than one flow at each location, they were numbered from bottom to top. It is important to emphasize, that sometimes the different flows on one hill are far away from each other. In that case, they have different GPS-coordinates (see Tab. 1) and each position is marked in Fig. 1. At Fagradallsfjall, the flows have the same coordinates, but different altitudes. Although not all flows are consecutive, their stratigraphic relationship is clear with FAG1 being the lowest and FAG13 the highest. At Nátthagakriki, the sampled flows are spatially apart. Only N3 is on top of N2 and N5 on top of N4. However, it is not clear, if for example N1 is the same flow as N6. Using similarities of paleomagnetic mean directions and intensities, some sites will be treated as contemporaneous later.

3 Dating

The age of the Skalamælifell excursion according to Levi et al. (1990) is 42.9±7.8 ka. It was projected to improve this, to eventually also obtain constraints on stratigraphy and on the length of the excursion. Based on macroscopic observations and K_2O contents, two samples, from BL and FAG, were selected for age determinations, as these flows were probably extruded before and after, respectively, the excursion (section 7). The technique used in this study is the unspiked K-Ar technique described in Charbit et al. (1998) and used to date other Laschamp samples from the type locality (Guillou et al., 2004). Unfortunately, all attempts to obtain reliable K-Ar ages failed. This is related both to the very young age and to the very low K contents in the samples, 0.191 and 0.183%, respectively in FAG and BL. As a consequence, the amount of radiogenic ^{40}Ar, in these samples, is below the limit of detection, which was previously calculated to be 0.15% (Scaillet and Guillou, 2004).

4 Rock magnetism

Rock magnetic measurements aimed to identify the magnetic mineralogy and domain state. Isothermal remanent magnetization (IRM) acquisition, isothermal backfield curves at room temperature, hysteresis loops, and thermomagnetic curves (T_{max} = 600 °C) were measured in that order. All measurements were conducted using a Variable Field Translation Balance (VFTB) and analyzed using the RockMag Analyzer software by Leonhardt (2006).

All basalts have similar rock magnetic properties. The tephra showed, however, a very different behavior. Thus, in the following it will be considered separate from the lavas.

All (normalized) IRM acquisition curves of the basalts are similar. At fields between 100 and 200 mT, 90% of the saturation remanence M_{rs} is reached and in almost all cases the remanence is already saturated below 300 mT. This shows that most of the magnetization is carried by low coercivity minerals like (titano-)magnetite. The same similiarity is observed for the normalized backfield curves, though values for the coercivity of remanence B_{cr} lie between 9.6 and 46 mT. The S_{300}-parameters (Bloemendal et al., 1992) are close to 1 (between 0.96 and 0.99; average 0.98) for all basaltic samples, which again reflects that the magnetization is carried by low coercive minerals. Hysteresis parameters plotted in a Day plot (Day et al., 1977), with domain state related boundaries according to Dunlop (2002), indicate a predominat distribution along the SD-MD mixing curve.

Examining the thermomagnetic curves lead to four groups with different characteristic Curie temperatures (Fig. 2), which were determined using the second derivative method (Tauxe, 1998). This method relies on the identification of maximum concave curvature within the measured data. The temperature at which this maximum occurred was used as an approximation for the Curie temperature (T_C). For ore microscopy (reflected light), two specimens of each thermomagnetic group were chosen (one of group 2a and one of 2b) and a Leitz Orthoplan pol microscope with a Nikon DXM 1200 digital camera, and air as well as immersion oil objectives with different magnification (20x and 50x) were used. To emphasize strong magnetic regions samples were covered with Ferrofluid. The specimens from the different thermomagnetic types also have particular appearances. The samples of group 1 have a single Curie temperature between 80 and 170 °C at the heating cycle and one at about 580 °C at the cooling curve (Fig. 2a). The low Curie temperature, and the fact, that only a few exsolution lamellae can be seen, suggest that these samples were not, or only to a small extent, oxidized. Additionally, there are also optical anisotropic grains, indicating the presence of ilmenites. The fact, that the cooling curve is much higher than the heating curve, shows that this titanomagnetite (e.g. TM60) was oxidized during heating in the laboratory. After heating it contains Ti-poor titanomagnetites or even magnetite. The second group has two Curie temperatures in the heating cycle, one at about 160 to 250 °C and one between 500 and 580 °C. This group splits again in two subgroups: The cooling curve of five samples is significantly higher than the heating curve (group 2a; Fig. 2b). The cooling curves of the five samples belonging to group 2b are close to the heating curves (Fig. 2c). The grains of FAG13-7C (group 2a) are very small (25 to 50 μm) and often have skeleton shape. FS2-6D (group 2b) contains many skeleton formed grains, but additionally also large ones (up to 130 μm). Some of the grains in both samples show exsolution lamellae of magnetite and ilmenite. The presence of grains with and without lamellae explains the existence of two different Curie temperatures. The different cooling curves of group 2a and 2b, and the easier high temperature oxidation in group 2a compared to group 2b, may be due to the smaller particles in group 2a and their higher surface/volume ratio. The two samples of group 3 have three Curie temperatures at the heating curve and only one at the cooling curve (Fig. 2d). Ore microscopy from group 3 specimens yielded different results: FAG5-2D shows many skeleton structures, while another sample, N5-5E, has mainly large ore minerals. In both cases some of the minerals show exsolution lamellae and some do not. Like in the case of group 2, this characteristic accounts for at least two of the three Curie temperatures. The third Curie temperature might be related to maghemitization or to only partial oxidation of some grains. However, shrinking cracks or other traces of maghemitization, could not be identified. Furthermore, the pristine olivine found in most samples indicates that no secondary alteration took place. Therefore, it is concluded that partial oxidation is responsible fot the third Curie temperature in this group. Only a single Curie temperature at about 500 to 580 °C and almost reversible heating/cooling cycles are typical for the samples of group 4 (Fig. 2e). Almost all grains of specimens from Group 4 have exsolution lamellae. The grain sizes strongly vary from about 20 μm to about 150 μm. In all cases the grains again have the typical oktahedral angles, and skeletons are common. Additionally ilmenite is present in both samples. The high Curie temperature is due to the highly oxidized grains.

In all experiments, the tephra behaves completely different than the basalts. IRM and backfield measurements indicate the presence of a high coercive fraction ($S_{300} = 0.88$), but as the remanence reaches saturation at about 500 mT, hematite or goethite cannot be the remanence carriers. The hysteresis loop of TE1-7D shows that the tephra has only a very small content of ferro(i)magnetic particles and is dominated by paramagnetism. Stepwise thermal demagnetization of tephra specimens revealed a blocking temperature between 150 and 250 °C. Thus, the tephra consists mainly of paramagnetic material, but also contains highly coercive minerals with a low blocking temperature. Unfortunately, ore microscopy could not be performed due to the granular character of the samples. Yet, blocking temperature and coercivity distribution indicate that either maghemite or an iron sulfide are remanence carriers. To obtain further insight, the coercivity variation in dependency of the heating step was investigated. Backfield measurements were conducted after heating to 20 °C, 200 °C, 420 °C, 550 °C, and 700 °C. B_{cr} decreases after heating to 420 °C. It is then reduced to only about 50% of the original value. This behavior could be explained by inversion of maghemite to magnetite, which is a quasi-continuous process above 300 °C (Krása and Matzka, 2007). The transformation of the iron sulphide pyrhotite to magnetite would show similar effects, but its inversion starts not until temperatures above 500 °C (Bina and Daly, 1994). Thus, the inversion of maghemite to magnetite is considered more probable. Nevertheless, due to the good fitting and stable paleodirectional data (subsection 7.1), it is very likely that the remanence was acquired during the excursion.

5 Paleodirections

All NRM measurements were carried out in the magnetically shielded room at the Niederlippach paleomagnetic laboratory of the University of Munich using a Molspin spinner magnetometer and a 2G Enterprises cryogen magnetometer. Half of the specimen were treated by stepwise thermal demagnetization (hereinafter referred to as TH), the other half by stepwise alternating field

(AF) demagnetization. TH demagnetization was done in a Schoenstedt furnace from 20 °C to 640°C in up to 17 heating steps. In addition to the NRM measurement, the susceptibility was measured after each heating step with a KLT-3 Minikappa bridge to detect changes of the mineral character. For AF demagnetization, a 2G Enterprises degausser system control was used and up to 13 steps from 0 to 200 mT were carried out to demagnetize the specimens. Paleodirections for the 178 specimens were calculated using principle component analysis (PCA; Tab. 1). In almost all cases the directions are very well defined by a best-fit line through more than five points (Fig. 3). If the maximum angular deviation (MAD) was more than 5°, the data was not further used. A viscous component (normal field direction) was usually removed at the 100 °C to 150 °C TH-step or the 10 mT AF-step. Only at some sites a secondary component beside this viscous component was observed. The site mean directions were determined using Fisher statistics (Fisher, 1953). The directional independence of flows, that are close to each other or which likely belong to one eruption, is tested using F-Distribution tests (e.g. at Nátthagakriki). If two sites are not different at a 95% significance level, it is assumed that they have recorded the same field and represent a single record. Therefore, they are combined and compared with the next flow following these. Using this technique repeatedly, groupings of sites are developed assuming that flows with similar directions are identical or contemporaneous (Tab. 1). When available, paleointensity results are considered for the similarity analysis (Tab. 2: FAG11 and FAG13).

All specimens from Fagradallsfjall show normal polarity and have somewhat right-handed declinations (e.g. Fig. 3a). A similar characteristic was observed by Kristjánsson (2003). However, as all lavas were likely extruded in a very short time interval, they do not represent sufficient time to average out secular variation and it is not clear if this right-handedness is at all due to long-term behavior of the geomagnetic field in the Brunhes chron (Levi et al., 1990). The sites at Festarfjall and Siglubergsháls (SI1, SI2, FS1) also show normal polarity, but with a strongly right-handed declination of 68.3° and inclination of 79.2° (Fig. 3e). FS2 even has a declination of 86.1° ($I = 75.7°$). These values correspond to those that Kristjánsson (2003) found at Borgarfjall ($D = 85°$, $I = 76°$). The mean direction of the base is between those of Fagradallsfjall, Festarfjall and Siglubergsháls, with a declination of 41.3°. The tephra has a declination of 317° and an inclination of 56.6° (Fig. 3b). As will be explained later (subsection 7.1), the onset of the excursion is represented by this paleo-direction.

Excursional directions, defined by virtual geomagnetic pole (VGP) latitudes more than 41.3° away from the geographic pole (McElhinny and McFadden, 1997), were found in ten flows. The sampled flow at Einbúi exhibits a declination of 280.1° and an inclination of 13.8° (Fig. 3c, d). At this site many specimens had to be analyzed using great circles (Fig. 3d). The previously reported excursional values ($D = 263.3°$, $I = -22.1°$, $k = 151.8$, $\alpha_{95} = 3.1°$, (Kristjánsson, 2003; Levi et al., 1990)) are almost identically observed at Bleikshóll (Fig. 3f). The specimens contain a relatively strong viscous overprint up to ca. 300 °C respectively 100 mT related to the weak NRM acquired during the excursional low-field state. The directions of the flows on Nátthagakriki fit some sites, whose geographical location Kristjánsson (2003) described as 'southwestern parts of Fagradallsfjall'. They all have similar directions with southerly declinations: VGP group N1, N2, N3, N5, N6: $D = 160.0°$ and $I = 64.1°$ (Fig. 3g) and N4: $D = 148.8°$ and $I = 60.0°$. It is not exactly clear, whether Kristjánsson measured samples of the same flows. Nevertheless, his results of $D = 167°$ and $I = 64°$ are very similar.

Directions that deviate from the normal/inverse polarity state are not necessarily due to reversals or excursions of the geomagnetic field, but may also be due to (partial) self-reversal as has been suggested by Néel (1951), who presented different theoretical mechanisms that could lead to this phenomenon. As mentioned before, Bonhommet and Babkine (1967) found intermediate paleomagnetic directions in samples from Laschamp and Olby. However, Heller (1980), Heller and Petersen (1982) and Krása et al. (2005) demonstrated that some remanence carriers in samples from Olby exhibit complete or partial self-reversal. Hence, samples from the excursional and normal polarity sites at Iceland were tested for this phenomenon. The samples were continuously thermally demagnetized in up to five subsequent measurement steps with increasing temperature in an high-temperature spinner magnetometer (HOTSPIN) (Matzka, 2001) at the Niederlippach paleomagnetic laboratory. This method allows for monitoring reversibility of heating/cooling cycles. In addition to NRM(T) intensity plots (Fig. 4a, c), directional plots of the core coordinates x and z, where the start of the respective heating cycles is labeled, can be drawn (Fig. 4b, d). FAG11-4F is a typical non self-reversing specimen. There is no maximum in the NRM(T) intensity plot (Fig. 4a) and, besides a small viscous overprint, only one linear directional trend to the origin can be observed (Fig. 4b). (Partial) self-reversing samples show a reversible peak at the same temperature of the HOTSPIN heating and cooling cycles (Fig. 4c). If self-reversal behavior also affects the paleodirection, two different directional trends are observed (one that could be observed also at stepwise demagnetization, i.e. measuring at 20 °C, and another one for the peak in the NRM(T) plot). It was found, that none of the excursional sites from Bleikshóll and Einbúi shows self-reversal. At Nátthagakriki only N6-4D shows partial self-reversal behavior, but it still has a stable direction with only one linear trend to the origin (Fig. 4c, d). Additionally, both samples from the Siglubergsháls flows and also specimen FS2-6C exhibit partial self-reversal with, however, again, stable directions. All specimens showing partial self-reversal are of thermomagnetic group 2b. The decrease of M_r in the characteristic manner of partial self-reversal is not observed in the respective $M_s(T)$ curves, and thus is not controlled by the temperature dependence of saturation magnetization. As the effect occurs during heating and cooling, it is probably caused by the blocking of the thermal remanent magnetization (TRM). The data for the different samples show that the remanences of the two carriers are antiparallel, i.e., that the angular difference is 180°. Hence, the remanence of the low-temperature component is coupled to the high-temperature component. It has been observed that the temperature of the maximum in the NRM(T) plot is always below the respective first Curie temperature of the sample; thus, it is probable that the low-temperature reversed remanence is carried by the magnetic phase with the lower T_c, which is the primary unoxidized titanomagnetite. Both, the mostly non self-reversing samples and the stable direction of N6-4D (Fig. 4c, d), which exhibits partial self-reversal, suggest that the Skalamælifell excursion is a real feature of the geomagnetic field.

6 Paleointensities

All paleointensity determinations were conducted in a MMTD20 thermal demagnetizer. Specimens for the Thellier experiments (Thellier and Thellier, 1959) were chosen due to high coercivity (AF demagnetization: medium destructive field > 20 mT) and small changes of susceptibility at thermal demagnetizations. Laboratory fields of 30 μT with a field accuracy of 0.1 μT were used for all measurements and applied during heating and cooling. Intensity determinations were performed with the modified Thellier-technique MT4 (Leonhardt et al., 2004a), which is a zero-field first method that includes the commonly used pTRM* (partial thermoremanence) check (Coe, 1967), additivity checks (Krása et al., 2003), and pTRM*-tail checks (Riisager and Riisager, 2001). For Thellier-type experiments pTRM acquisition is different to the traditional pTRM definition, as the maximum temperature at which the laboratory field is applied is not reached from T_C. Therefore, pTRM* is used as an abbreviation. Directional differences between the applied field and the NRM of the pTRM*-tail check are taken into account according to Leonhardt et al. (2004b). The pTRM* checks were conducted "in-field" after the demagnetization step with a laboratory field applied during heating and cooling. All determinations were analyzed using the ThellierTool4.11 software (Leonhardt et al., 2004a). This software allows full vector analysis as well as the application of a check correction (Valet et al., 1996; Leonhardt et al., 2003) and provides a default set of acceptance criteria, which is as follows: For the linear fit at least 5 subsequent data points have to be used, comprising at least a 30% fraction of the NRM (f), its standard deviation has to be less than 0.15 and the MAD less than 15. Only directions with α_{95} smaller than 15 are accepted. As no alteration should occur, pTRM checks have to be within 7% of the original TRM value ($\delta(CK)$) and the cumulative check difference ($\delta(pal)$) has to be less than 10%. Further only relative errors of the additivity checks ($\delta(AC)$) up to 10% are accepted, while the relative intensity difference between the remaining NRM and the respective pTRM*tail-check ($\delta(TR)$) has to be within 15% and the true pTRM*-tail ($\delta(t*)$) below 5%. Additionally paleointensity determinations that failed some of the acceptance criteria, but matched other data from the same site which passed the criteria, were used.

For some specimen check correction was applied to analyze the data, because of deviating pTRM-checks, which are probably connected with formation of new magnetic particles. By using the cumulative pTRM check difference the contribution of this new phase could be subtracted. After check correction additivity checks fall on the corresponding pTRM value suggesting that TRM properties of the original magnetic content are preserved and check correction is successful. To exclude biasing effects, check corrected data were compared with other data from the same site. Samples from FAG13 could be analyzed only using check corrected plots. However, the two results are consistent and for the check corrected Arai plot of FAG13-6E, it was possible to analyze the whole temperature interval. Thus, the results are considered reliable. The Thellier experiments of most samples from BL2, FAG7, FAG8, FAG12, N1, N2, N5, SI1 and SI2 yielded no results due to uncorrectable alteration and MD effects. The paleointensity results of each site were averaged and also a standard deviation was calculated, using the quality factor q (Coe et al., 1978) for weighting. Furthermore, a mean paleointensity and a standard deviation (arithmetic mean of different sites) were determined for the directional groups. All results and the different quality parameters are listed in Tab. 2.

To check for a possible influence of magnetic anisotropy, anisotropy of the magnetic susceptibility was measured using a KLY-2 Kappa bridge, indicating a negligible effect as the overall values for the anisotropy factor $P < 1.01$ are small.

The normal sites yield paleointensities similar to the present-day field value of Iceland, which is 52.3 μT. The base (B1) recorded a weighted mean paleointensity of 59.3$\pm$4.1 μT (Fig. 5a). FAG11 shows a weighted mean intensity of 47.8$\pm$1.1 μT. This paleointensity determinaton is mainly based on check corrected results, which, however, are absolutely consistent with the non-corrected result of FAG11-1C. The two check corrected determinations of site FAG13 result in a mean paleointensity of 33.8±0.2 μT, which is considerably smaller than the paleointensity at FAG11. The flows at Siglubergsháls and Festarfjall yield a paleointensity of about 30 μT (27.4 μT; 28.5±2.2 μT). The intensities of the excursional sites BL1 and BL3 (Fig. 5b), 5.2±0.2 μT and 4.0±0.4 μT respectively, are only about 1/10 the intensity of the normal sites. The data within these sites are were well defined and match each other. The flows at Nátthagakriki have also a low paleointensity, which is only about 1/3 of the intensity prior to the excursion, as can be seen by the mean value of the VGP group (N1, N2, N6): 19.9±2.4 μT. Taken together, specimens from unit N1 and N2 yielded just two reliable results. The weighted mean intensity of N6, 18.4±0.4 μT, is the only one that is defined by four specimens (Fig. 5c), but the results of the two specimens at the sites N1 and N2 are consistent with the data at N6. Paleointensity of these flows is significantly higher than the one recorded by the flows at Bleikshóll, but still less than half the paleointensity at sites with normal directions.

7 Discussion

It has been outlined before, that the paleodirectional data is very consistent and reliable. In almost all cases the PCA-analysis resulted in a small MAD, and the comparison of sun and magnetic compass yielded no difference. After removal of minor VRMs most site mean directions are very well defined with $\alpha_{95} < 10°$ and $k > 100$. Although the remanence carriers of the tephra could not be unambiguously identified, the direction is still considered reliable due to its good agreement with other data (subsection 7.1). Self-reversal experiments led to the conclusion that the observed excursion is not due to partial self-reversal, but a real feature of the geomagnetic field. Only one excursional specimen exhibits partial self-reversal, and continuous thermal demagnetization shows that its direction is not affected. The paleointensity data, tested with various checks, meet strict classification criteria, and show consistent within-site results underlining their high quality.

7.1 Comparison with igneous sections and marine records

Fig. 6a shows the Skalamælifell geomagnetic field excursion VGPs together with those found by previous studies on Iceland and at Laschamp. It is obvious that the Bleikshóll data fits the results of Kristjánsson (2003) and Levi et al. (1990) perfectly. The VGPs of the flows at Laschamp and Olby lay further south at latitudes of -46° and -56° (Roperch et al., 1988). However, this difference has already been recognized by Kristjánsson (2003) and Levi et al. (1990), who suggested that it might be due to non-dipole contributions to the geomagnetic field, small age differences, or local/regional crustal magnetic anomalies. The VGP of the Louchadière lava flow as found by Chauvin et al. (1989) is closer to the VGPs of Nátthagakriki. As mentioned before, the stratigraphy of the Reykjanes area is quite difficult. Only a few sites and directional groups, whose flows are consecutive, can be connected a priori (Fig. 6a). Comparing the VGPs with sedimentary records helps to establish a chronology between some of the other flows. First, the VGPs are plotted together with data from the ODP (Ocean drilling program) site 919 in the Irminger Basin (62.67°N, 37.46°W) (Channell, 2006) (Fig. 6b). This site was chosen due to its vicinity to Iceland. A new and even closer record (PS2644-5) shows a very similar VGP path (Laj et al., 2006) (Fig. 6c). The tephra and Einbúi VGPs plot almost perfectly on the southward VGP path of the ODP 919 record along the eastern coast of America, and the data from Bleikshóll fits in well, too (south-east Pacific). The small deflection may be due to the geographical distance between ODP site 919 and the sampled sites. Laj et al. (2006) studied some new records of the Laschamp excursion and compared them also to other records by Lund et al. (2005). The records show clockwise loops, which can also be seen at ODP site 919. Many VGP paths go south over the Pacific, then west to Africa, and back north over Europe (Fig. 6c). Thus, one might suggest that the VGPs in North Africa (Nátthagakriki) follow those in the Eastern Pacific (Bleikshóll). As mentioned before, field observations suggest that the base (B1) is the oldest part of the area while younger flows of Fagradallsfjall overlie the older ones of Nátthagakriki. The relationship of the flows from Siglubergsháls and Festarfjall to the other flows, however, cannot be solved with the available paleodirectional and -intensity data. The VGP loops of Laj et al. (2006), as well as the paleointensity values between Nátthagakriki and Fagradallsfjall, might suggest that the flows at Siglubergsháls and Festarfjall follow those at Nátthagakriki. However, more data is needed to prove this suggestion. Therefore, the sites FS1, FS2, SI1 and SI2 are not included in the following stratigraphy. Fig. 6d shows the suggested VGP path. The time span between the individual flows is unclear due to the sporadic nature of volcanic eruptions. There might have been changes of the geomagnetic field between different events that are not recorded and for example the base could also be much older. Nevertheless, it is at least likely that the excursion units represent only a few hundred years. Levi et al. (1990) suggested that their observed excursional lavas, which all show transitional VGPs close to South America, were extruded during a short time interval, due to their almost identical paleomagnetic directions and their similar chemical and petrologic features. As the excursion units are mostly elevated in the order of 100 m, which has been observed to occur in southwestern Iceland in less than 100 years, Levi et al. (1990) further suggested that the lavas were extruded in no more than several hundred years. This opinion is also supported by Kristjánsson (2003).

The previous intermediate paleointensity values by Marshall et al. (1988) and Levi et al. (1990) are quite similar to the paleointensities at Bleikshóll. Marshall et al. (1988), who could analyze only six excursional samples, of which four yielded reliable results, found paleointensities in a range from 3.4 to 4.6 μT (mean 4.3±0.6 μT). From their five reliable results of normal samples, they got a wider range between 22 μT and 47 μT (mean 30 μT). Levi et al. (1990) selected eight excursion specimens for paleointensity studies, which yielded a weighted mean paleointensity of 4.2±0.2 μT. They determined no normal paleointensity values. Our paleointensity at BL3 (4.0±0.4 μT) is statistically indistinguishable from the earlier data and thus confirms the former results, while the one at BL1 (5.2±0.2 μT) is slightly higher, probably due to a slight difference in age. The paleointensity determinations of the Nátthagakriki flows (arithmetic mean: 19.9±2.4 μT) give new results for an excursional unit that have not been reported before. Our paleointensity values of the normal flows range between 27.4 μT and 59.3±4.1 μT and are slightly larger than those reported by Marshall et al. (1988). Roperch et al. (1988) performed paleointensity measurements at the Laschamp and Olby flows in France. Their measurements gave an intensity of 7.7±1.6 μT, while the measurements of Chauvin et al. (1989) yielded a paleointensity of 12.9±3.3 μT for the excursional flow at Louchadière. Sedimentary records reflect the low paleointensities during the Laschamp excursion, too (Channell, 2006; Lund et al., 2005).

7.2 Local and global field state during the excursion

In Fig. 7a, declination and inclination as well as paleointensity are plotted versus the established stratigraphy. It is important that no absolute time can be assigned and that the periods between the records may differ significantly. During the excursion a massive change of declination and inclination as well as a decrease of intensity is observed. The start of the excursion is recorded by the tephra, which shows a strong change of declination, but not in inclination. This is followed by shallow positive and negative inclination values and declination values of about -90° (E1, DG1: BL1 and BL2, BL3). An intensity measurement of site E1 was not possible. However, the flows at Bleikshóll show that the intensity decreases to only 1/10 of its original value. Towards the end of the excursion, southerly declination values are observed, while inclination already is positive and steep again (DG2: N1, N2, N3, N4, N5, N6). At this time intensity regained about 1/3 of its value before the excursion. The time after the excursion is recorded by the flows at Fagradallsfjall. Their declination seems to be quite stable, inclination, however, changes by more than 15°. Intensity after the excursion is some 10 μT smaller than before it, an effect that has already been observed by Marshall et al. (1988). Between FAG11 and FAG13 paleointensity again decreases by almost 15 μT. Fig. 7b shows the variation of declination, inclination and a paleointensity proxy for ODP site 919. Data from Iceland and ODP site 919 agree very well, which confirms the established stratigraphic order. Although no absolute paleointensity values can be assigned for the PI proxy, a qualitative comparison with the icelandic data 919 (Channell, 2006) shows that the marine sedimentary record has a higher intensity towards the end of the excursion, too (Fig. 7b).

Different models were developed in the past to describe excursions. Generally the idea is held, that the noticeable intensity minima, which coincide with directional excursions, imply an emergence of non-dipole geomagnetic components (Merrill and McElhinny, 1994). Based on the 40° difference between the VGPs of Laschamp/Olby and Skalamælifell and the assumption of simultaneous records, Levi et al. (1990) supported this hypothesis, arguing that the low latitude VGPs are related to a decrease of the axial dipole and a substantial contribution by higher order multipole terms. The same idea was proposed earlier by Marshall et al. (1988), who suggested that the non-dipole fields were of about historical intensity while the axial dipole was unusually weak. In the various studies of sedimentary Laschamp records diverse theories were developed to explain a decrease of the axial dipole. A different idea than the one by Merrill and McElhinny (1994) was postulated by Laj et al. (2006). As mentioned before, they observed strikingly similar excursion loops with a simple structure for five new records of the Laschamp excursion. Thus, they suggested that the geomagnetic field during the excursion predominately had a relatively simple geometry. The excursion loops would have to be much more different, if non-dipole fields were dominating. In order to account for the reduced intensity, they proposed a decrease of the axial dipole, a substantial equatorial dipole and a simultaneously reduced non-dipole field relative to the axial dipole. Our data, which originates from the Northern hemisphere close to site locations used by Laj et al. (2006) agree well to this earlier interpretaion. Neveretheless, a contribution of multipolar terms, at least for a brief time interval, is necessary to explain the directional deviations between Laschamp/Olby (Roperch et al., 1988), New Zealand (Cassata et al., 2008) and Skalamælifell. These observations are supported by a global field model of the Laschamp excursion (Leonhardt et al., 2009), in which the Bayesian inversion method of Leonhardt and Fabian (2007) is used to establish a model of the geomagnetic field during the Laschamp excursion, by incorporating the results of the Skalamælifell data. It shows decreasing dipolar and non-dipolar terms with equatorial dipolar terms dominating the onset of the excursion and a non-dipolar dominance for a brief time interval during the excursion.

8 Conclusion

The Laschamp excursion was sampled at 29 sites on Reykjanes Peninsula, Iceland and a sequence of absolute paleointensities was firstly developed during this study. Paleodirections were determined using stepwise demagnetization methods. Overall, the directional determinations are characterized by very small uncertainties. Ten of the 28 sampled lava flows and a tephra layer recorded the Skalamælifell excursion. VGPs are found in the East Pacific: One north and three south of the equator. Six other intermediate VGPs are located in West Africa. Rock magnetic investigations show that the main remanence carriers of the basalts are (titano-)magnetites with different degrees of high temperature oxidation. The rock magnetic features of the tephra could not be solved unambiguously. Partial self-reversal was observed for four specimens that show two Curie temperatures and reversible heating/cooling cycles. Only one excursional specimen belongs to this thermomagnetic group and like the other three specimens its paleodirection was unaffected by the partial self-reversal. 52 samples from 16 flows were subjected to Thellier-type paleointensity determinations, which include tests to check for alteration and multidomain effects. Determinations of anisotropy of magnetic susceptibility indicate negligible magnetic anisotropy. Reliable paleointensity data were obtained for ten of the 29 sites. The paleointensities of the excursional sites have values of about 4 to 5 μT, about 1/10 of the intensity of the normal polarity flows (27.4 to 59.3±4.1 μT). Towards the end of the excursion, but still during an intermediate directional state with VGPs over Africa, paleointensity regained about 1/3 of its original value (19.9±2.4 μT). A comparison of the paleointensity data with the results of previous studies at the same sampling location gives a very consistent picture, as all records show almost identical intensity values during the Skalamælifell excursion. Stratigraphic relationships on Reykjanes Peninsula, Iceland are quite difficult as the different volcanic structures are isolated. However, a tentative stratigraphic relationship between 25 sites prior to, during and after the Skalamælifell excursion was established by comparing them with paleomagnetic data from nearby marine sedimentary records. Only VGPs from four normal polarity flows could not be matched unambiguously to those of the marine records. Taken together, our results support the theory of Laj et al. (2006), that the geomagnetic field had a simple transitional field geometry at least during the onset of the Laschamp excursion. The data are best explained by a decrease of the axial dipole relative to the equatorial dipole that was accompanied by a considerably reduced non-dipole field, which is further supported by geomagnetic field modelling (Leonhardt et al., 2009).

Acknowledgements

We gratefully acknowledge Leo Kristjánsson for sharing his fundamental knowledge about geology and paleomagnetism on Iceland. We also thank Hervé Guillou and Sebastien Nomade whose time consuming dating experiments were unfortunately unsuccessful. We further want to thank Jim Channell, Carlo Laj and Shaul Levi who provided their sedimentary data. Funding was provided by DFG grants Wi1828/3-1 and So72/67-4.

References

Benson, L., Liddicoat, J. C., Smoot, J., Sarna-Wojcicki, A. M., Negrini, R. M., Lund, S., 2003. Age of the Mono Lake excursion and associated tephra. Quarternary Science Reviews 22, 135–140.

Bina, M., Daly, L., 1994. Mineralogical change and self-reversed magnetizations in pyrrhotite resulting from partial oxidation; geophysical implications. Phys. Earth Planet. Inter. 85, 83–99.

Bloemendal, J., King, J. W., Hall, F. R., Doh, S.-J., 1992. Rock magnetism of late Neogene and Pleistocene deep-sea sediments: Relationship of sediment source, diagenetic processes and sediment lithology. J. Geophys. Res. 97, 4361–4375.

Bonhommet, N., Babkine, J., 1967. Sur la présence d'aimentations inversées dans la Chaine des Puys. Comptes rendus de l'Académie des sciences Paris 264, 92–94.

Cassata, W., Singer, B. S., Cassidy, J., 2008. Laschamp and Mono Lake geomagnetic excursions recorded in New Zealand. Earth Planet. Sci. Lett. 268, 76–88.

Channell, J., 2006. Late Brunhes polarity excursions (Mono Lake, Laschamp, Iceland Basin and Pringle Falls) recorded at ODP Site 919 (Irminger Basin). Earth Planet. Sci. Lett. 244, 378–393.

Charbit, S., Guillou, H., Turpin, L., 1998. Cross calibration of K-Ar standard minerals using an unspiked Ar measurement technique. Chemical Geology

150 (1-2), 147–159.

Chauvin, A., Duncan, R., Bonhommet, N., Levi, S., 1989. Paleointensity of the Earth's magnetic field and K-Ar dating of the Louchadière volcanic flow (Central France). New evidence for the Laschamp excursion. Geophys. Res. Lett. 16, 1189–1192.

Coe, R. S., 1967. Palaeointensity of the Earth's magnetic field determined from tertiary and quaternary rocks. J. Geophys. Res. 72, 3247–3262.

Coe, R. S., Grommé, S., Mankinen, E. A., 1978. Geomagnetic paleointensities from radiocarbon-dated lava flows on Hawaii and the question of the Pacific nondipol low. J. Geophys. Res. 83, 1740–1756.

Day, R., Fuller, M. D., Schmidt, V. A., 1977. Hysteresis properties of titanomagnetites: Grain size and composition dependence. Phys. Earth Planet. Inter. 13, 260–266.

Dunlop, D., 2002. Theory and application of the Day plot (M_{rs}/M_s versus H_{cr}/H_c) 1. Theoretical curves and tests using titanomagnetite data. J. Geophys. Res. 107, 10.1029/2001JB000486.

Fisher, R. A., 1953. Dispersion on a sphere. Proc. R. Soc. London A 217, 295–305.

Gubbins, D., 1999. The distinction between geomagnetic excursions and reversals. Geophys. J. Int. 137, F1–F3.

Guillou, H., Singer, B., Laj, C., Kissel, C., Scaillet, S., Jicha, B., 2004. On the age of the Laschamp geomagnetic excursion. epsl 227, 331–343.

Heller, F., 1980. Self-reversal of natural remanent magnetization in the Olby Laschamp lavas. Nature 284, 334–335.

Heller, F., Petersen, N., 1982. Self-reversal explanation for the Laschamp/Olby geomagnetic field excursion. Phys. Earth Planet. Inter. 30, 358–372.

Krása, D., Heunemann, C., Leonhardt, R., Petersen, N., 2003. Experimental procedure to detect multidomain remanence during Thellier-Thellier experiments. Phys. Chem. Earth 28, 681–687.

Krása, D., Matzka, J., 2007. Inversion of titanomaghemite in oceanic basalt during heating. Phys. Earth Planet. Inter. 160, 169–179.

Krása, D., Shcherbakov, V. P., Kunzmann, T., Petersen, N., 2005. Self-reversal of remanent magnetization in basalts due to partially oxidized titanomagnetites. Geophys. J. Int. 162, 115–136.

Kristjánsson, L., 2003. Paleomagnetic observation on Late Quaternary basalts around Reykjavik and on the Reykjanes peninsula, SW-Iceland. Jökull 52, 21–32.

Kristjánsson, L., Gudmundsson, L., 1980. Geomagnetic excursion in late-glacial basalt outcrops in South-Western Iceland. Geophys. Res. Lett. 7, 337–340.

Laj, C., Channel, J. E. T., 2007. Treatise in Geophysics, Vol. 5. Elsevier, Ch. Geomagnetic excursions, pp. 373–416.

Laj, C., Kissel, C., Roberts, A., 2006. Geomagnetic field behavior during the Iceland Basin and Laschamp geomagnetic excursions: A simple transitional field geometry? Geochem. Geophys. Geosys. 7, doi:10.1029/2005GC001122.

Leonhardt, R., 2006. Analyzing rock magnetic measurements: The RockMagAnalyzer 1.0 software. Comp. Geosci. 32, 1420–1431.

Leonhardt, R., Fabian, K., 2007. Paleomagnetic reconstruction of the global geomagnetic field evolution during the Matuyama/Brunhes transition: Iterative Bayesian inversion and independent verification. Earth Planet. Sci. Lett. 253, 172–195.

Leonhardt, R., Fabian, K., Winklhofer, M., Ferk, A., Laj, C., Kissel, C., 2009. Geomagnetic field evolution during the Laschamp excursion. Earth Planet. Sci. Lett. 278, 87–95.

Leonhardt, R., Heunemann, C., Krása, D., 2004a. Analyzing absolute paleointensity determinations: Acceptance criteria and the software ThellierTool4.0. Geochem. Geophys. Geosys. 5, Q12016, doi:10.1029/2004GC000807.

Leonhardt, R., Krása, D., Coe, R. S., 2004b. Multidomain behavior during Thellier paleointensity experiments: A phenomenological model. Phys. Earth Planet. Inter. 147, 127–140.

Leonhardt, R., Matzka, J., Menor, E. A., 2003. Absolute paleointensities and paleodirections from Fernando de Noronha, Brazil. Phys. Earth Planet. Inter. 139, 285–303.

Levi, S., Audunsson, H., Duncan, R. A., Kristjansson, L., Gillot, P.-Y., Jakobsson, S. P., 1990. Late Pleistocene geomagnetic excursion in Icelandic lavs: confirmation of the Laschamp excursion. Earth Planet. Sci. Lett. 96, 443–457.

Levi, S., Karlin, R., 1989. A sixty thousand year paleomagnetic record from Gulf of California sediments: secular variation, late Quaternary excursions and geomagnetic implications. Earth Planet. Sci. Lett. 92, 219–233.

Lund, S., Schwartz, M., Keigwin, L., Johnson, T., 2005. Deep-sea sediment records of the Laschamp geomagnetic field excursion (similar to 41,000 calendar years before present). J. Geophys. Res. 110.

Lund, S., Stoner, J., Channell, J., Acton, G., 2006. A summary of Brunhes paleomagnetic field variability recorded in Ocean Drilling Program cores. Phys. Earth Planet. Inter. 156, 194–204.

Marshall, M., Chauvin, A., Bonhommet, N., 1988. Preliminary paleointensity measurements and detailed magnetic analysis of basalts from the Skalamaelifell excursion, southwest Iceland. J. Geophys. Res. 93, 11681–11698.

Matzka, J., 2001. Besondere magnetische Eigenschaften der Ozeanbasalte im

Altersbereich 10 bis 40 Ma. Ph.D. thesis, Ludwig-Maximilians-Universitt Munich.

McElhinny, M. W., McFadden, P. L., 1997. Palaeosecular variation over the past 5 Myr based on a new generalized database. Geophys. J. Int. 131, 240–252.

Merrill, R., McElhinny, M., 1994. Geomagnetic field stability: Reversal events and excursions. Earth Planet. Sci. Lett. 121, 57–69.

Néel, L., 1951. L'inversion de l'aimantation permanente des roches. Annales de Géophysique 7, 90–102.

Prévot, M., Mankinen, E. A., Coe, R. S., Grommé, S., 1985. The Steens Mountain (Oregon) geomagnetic polarity transition 2. Field intensity variations and discussion of reversal models. J. Geophys. Res. 90, 10417–10448.

Riisager, P., Riisager, J., 2001. Detecting multidomain magnetic grains in Thellier paleointensity experiments. Phys. Earth Planet. Inter. 125, 111–117.

Roperch, P., Bonhommet, N., Levi, S., 1988. Paleointensity of the Earth's magnetic field during the Laschamp excursion and its geomagnetic implications. Earth Planet. Sci. Lett. 88, 209–219.

Scaillet, S., Guillou, H., Apr. 2004. A critical evaluation of young (near-zero) K-Ar ages. Earth and Planetary Science Letters 220 (3-4), 265–275.

Tauxe, L., 1998. Paleomagnetic principles and practice. Kluwer Academic Publishers, London.

Thellier, E., Thellier, O., 1959. Sur l'intensité du champ magnétique terrestre dans le passé historique et géologique. Ann. Géophys. 15, 285–376.

Valet, J.-P., Brassart, J., Le Meur, I., Soler, V., Quidelleur, X., Tric, E., Gillot, P.-Y., 1996. Absolute paleointensity and magnetomineralogical changes. J. Geophys. Res. 101 (B11), 25029–25044.

Valet, J.-P., Plenier, G., Herrero-Bervera, E., 2008. Geomagnetic excursions reflect an aborted polarity state. Earth Planet. Sci. Lett. 274, 472–478.

Fig. 1. Topographic map showing the sampling area. Sampled sites are marked. Inlet: The black square on the map of Iceland marks the location of the sampling area. Topographic map: Stadfrædikort, map sheet 1512-I, 1:50,000, Landmælingar Islands and American DMA, 1990.

Fig. 2. Ore microscopy images with 50x oil lens (a, c, e with Fe-Fluid, b and d without) and thermomagnetic curves of the four different groups (group 2 splits in two subgroups).

Fig. 3. Orthogonal projections of some representative specimens of a, e) normal and c, f, g) excursional polarity. b) shows results from the tephra and d) a stereographic projection of a great circle analysis. Open symbols correspond to the vertical component, closed symbols to the horizontal component.

Fig. 4. Continuous thermal demagnetization curves and directional plots (x, z are core coordinates) of a, b) FAG11-4F which shows no partial self-reversal and c, d) N6-4D which is partial self-reversing. Different heating cycles are labeled.

Fig. 5. Three representative examples of accepted MT4 paleointensity determinations. Arai plots (Circles: pTRM/NRM values; Triangles: Alteration checks; squares: Additivity checks) and orthogonal projections (Open symbols: Vertical component; closed symbols: horizontal component) are shown and the paleointensity as determined from the slope of the straight line is given.

Fig. 6. a) VGPs as determined from our data (black) and VGPs from volcanic rocks of previous studies of the Laschamp excursion (grey). sc in the site name marks secondary components. Stratigraphic progression due to field evidence is emphasized. b) VGPs of Skalamælifell (black) together with those of ODP site 919 (Channell, 2006) (grey). c) Excursional VGP loops of different sedimentary records (Lund et al., 2005; Laj et al., 2006). d) Established VGP path (by correlation with b and c) at Skalamælifell. Locations are always indicated by bigger symbols: a) black: Skalamælifell, grey: Laschamp; b) black: Skalamælifell, grey: ODP 919, c) same symbol as VGPs but different colour (grey), d) star: Iceland.

Fig. 7. Declination, inclination and paleointensity trend for a) the suggested stratigraphical sequence at Iceland (vertical axis, which is valid for all three plots, shows the sequence of the flows) and b) ODP site 919. The grey background shows respective time intervals.

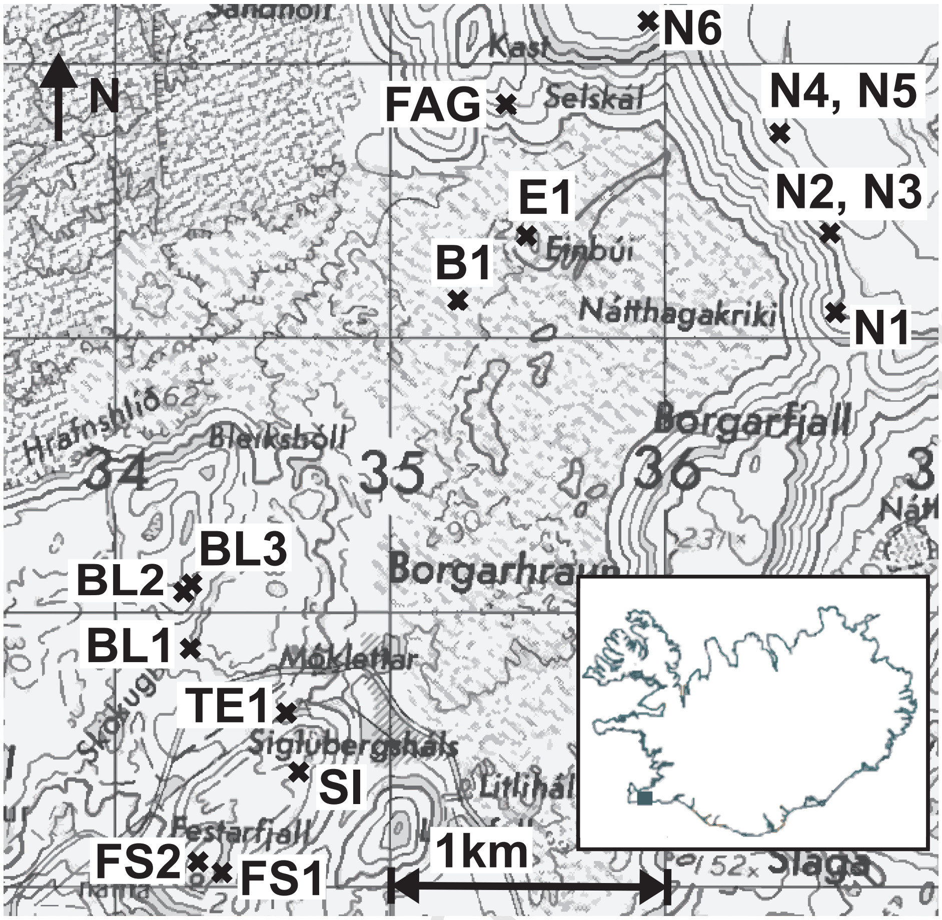
N
N6
FAG
N4, N5
E1
N2, N3
B1
N1
BL3
BL2
BL1
TE1
SI
FS2
FS1
1km
Kast
Selskál
Einbúi
Nátthagakriki
Borgarfjall
Bleiksholl
34
35
36
Borgarhraun
Móklettar
Siglubergsháls
Festarfjall
Litliháls

Figure 2

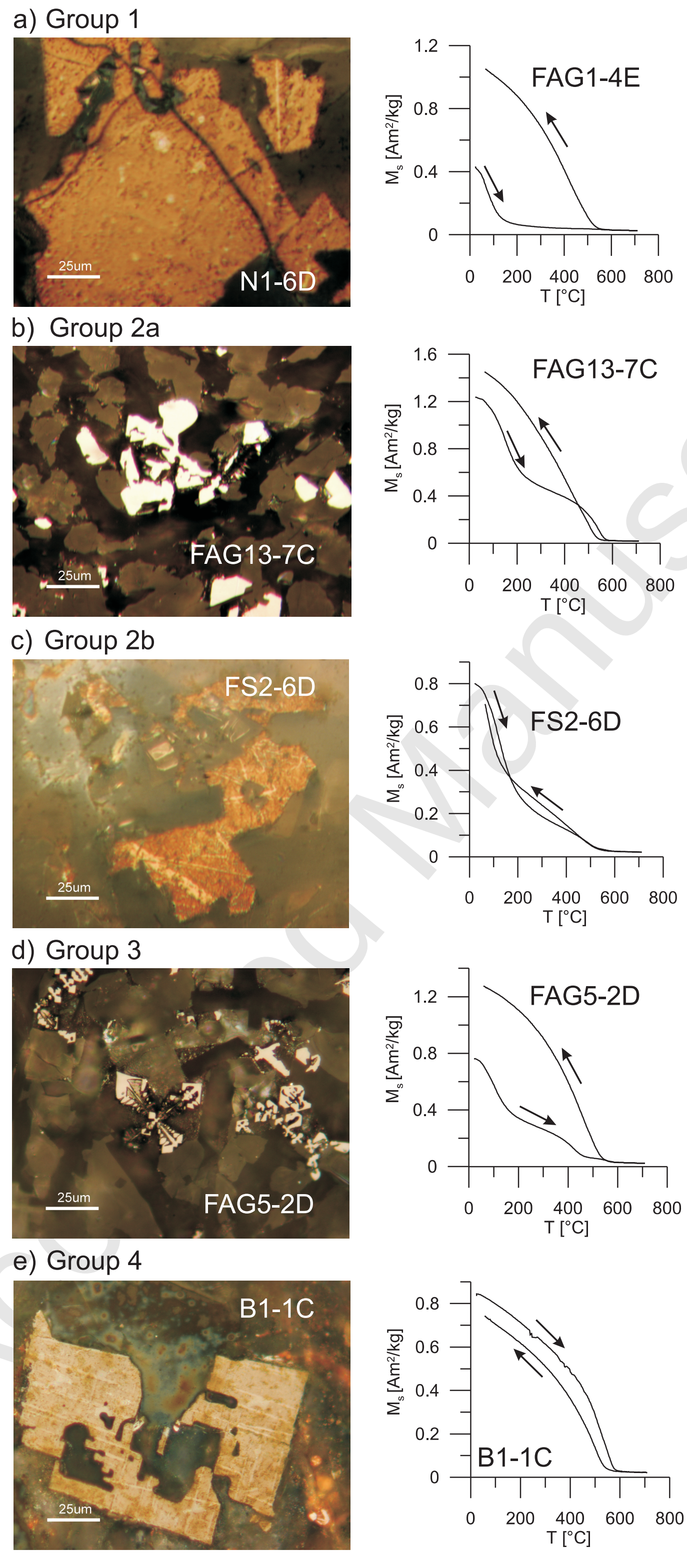
a) Group 1
25um
N1-6D
FAG1-4E
M_s [Am²/kg]
1.2
0.8
0.4
0
0 200 400 600 800
T [°C]
b) Group 2a
FAG13-7C
25um
FAG13-7C
1.6
1.2
0.8
0.4
0
M_s [Am²/kg]
0 200 400 600 800
T [°C]
c) Group 2b
FS2-6D
25um
FS2-6D
0.8
0.6
0.4
0.2
0
M_s [Am²/kg]
0 200 400 600 800
T [°C]
d) Group 3
25um
FAG5-2D
FAG5-2D
1.2
0.8
0.4
0
M_s [Am²/kg]
0 200 400 600 800
T [°C]
e) Group 4
B1-1C
25um
B1-1C
0.8
0.6
0.4
0.2
0
M_s [Am²/kg]
0 200 400 600 800
T [°C]

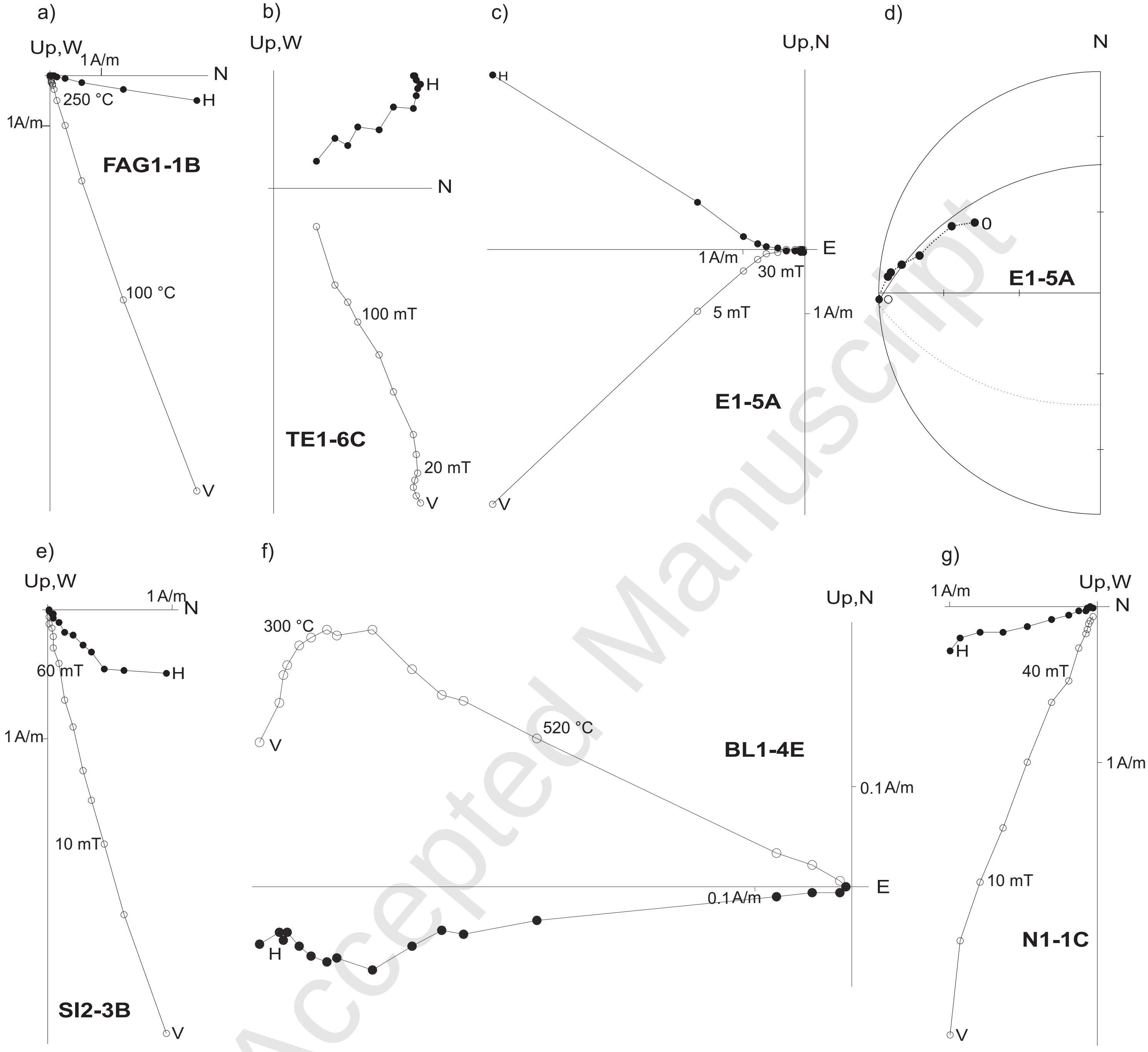
a)
Up,W
1 A/m
N
H
250 °C
1A/m
FAG1-1B
100 °C
V
b)
Up,W
H
N
100 mT
TE1-6C
20 mT
V
c)
Up,N
H
E
1 A/m
30 mT
5 mT
1 A/m
E1-5A
V
d)
N
0
E1-5A
O
e)
Up,W
1 A/m
N
60 mT
H
1 A/m
10 mT
SI2-3B
V
f)
Up,N
300 °C
V
520 °C
BL1-4E
0.1 A/m
E
0.1 A/m
H
g)
1 A/m
Up,W
N
H
40 mT
1 A/m
10 mT
N1-1C
V

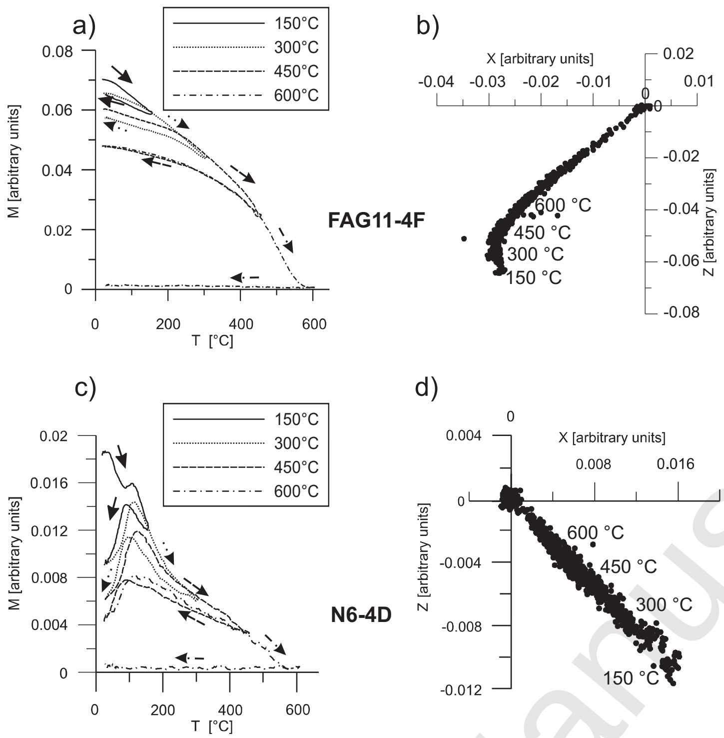
a)
150°C
300°C
450°C
600°C
M [arbitrary units]
T [°C]
b)
X [arbitrary units]
Z [arbitrary units]
600 °C
450 °C
300 °C
150 °C
FAG11-4F
c)
d)
N6-4D

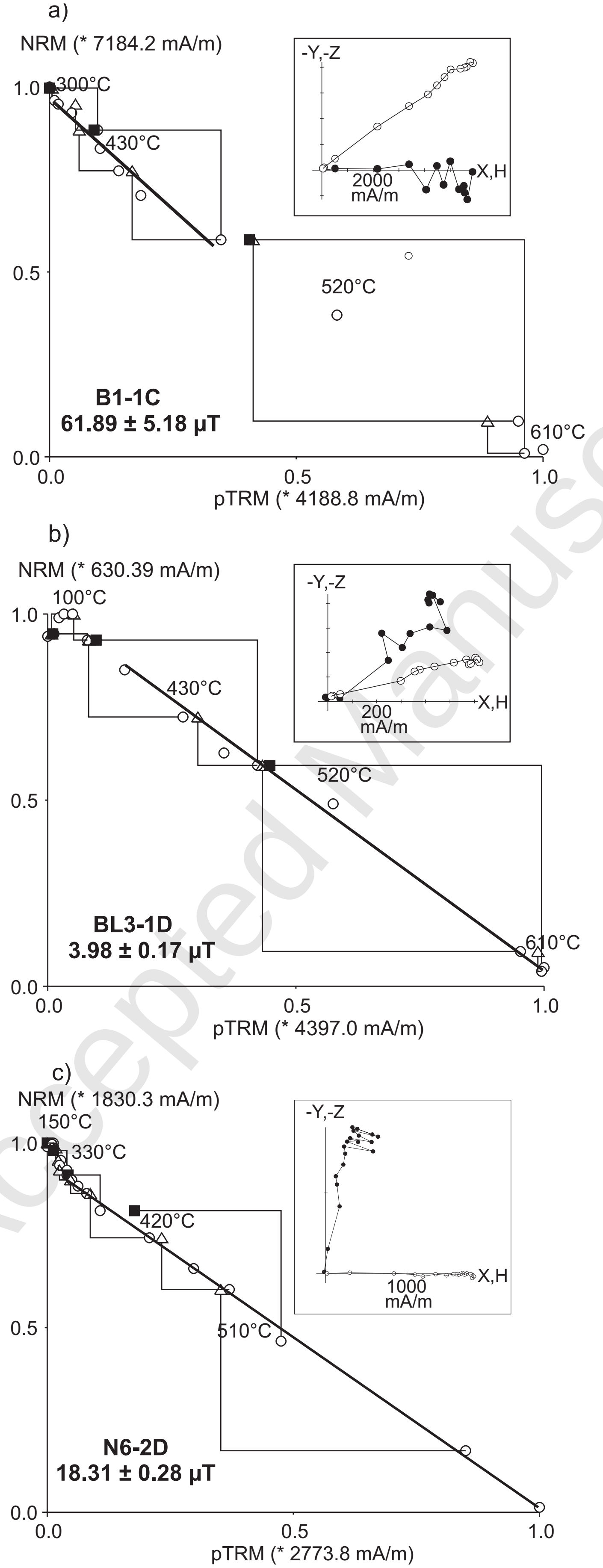
a)
NRM (* 7184.2 mA/m)
300°C
430°C
520°C
610°C
B1-1C
61.89 ± 5.18 µT
pTRM (* 4188.8 mA/m)
-Y,-Z
X,H
2000
mA/m
b)
NRM (* 630.39 mA/m)
100°C
430°C
520°C
610°C
BL3-1D
3.98 ± 0.17 µT
pTRM (* 4397.0 mA/m)
-Y,-Z
X,H
200
mA/m
c)
NRM (* 1830.3 mA/m)
150°C
330°C
420°C
510°C
N6-2D
18.31 ± 0.28 µT
pTRM (* 2773.8 mA/m)
-Y,-Z
X,H
1000
mA/m

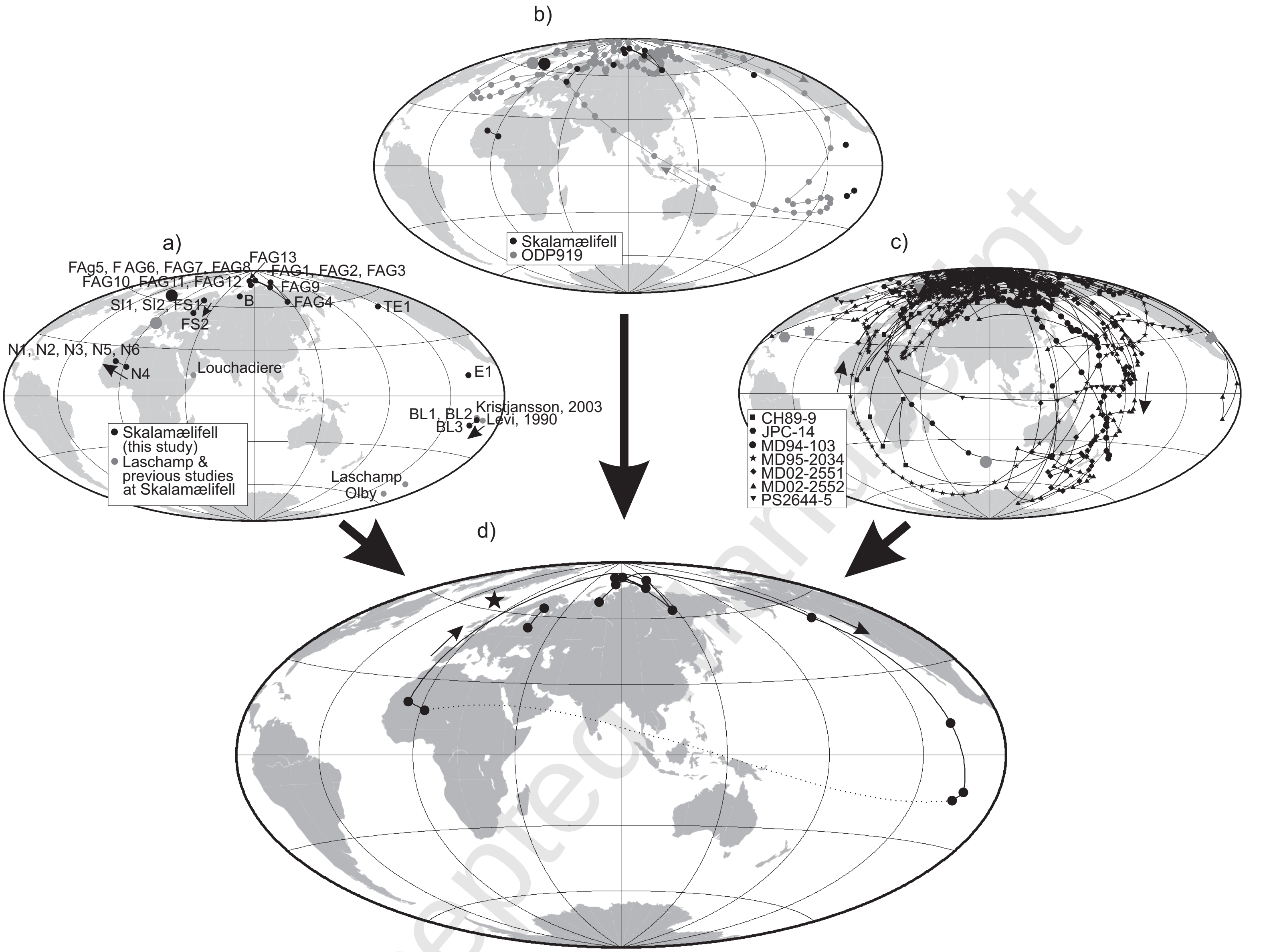
b)
Skalamælifell
ODP919
a)
FAg5, F AG6, FAG7, FAG8
FAG10, FAG11, FAG12
FAG13
FAG1, FAG2, FAG3
FAG9
FAG4
SI1, SI2, FS1
FS2
B
TE1
N1, N2, N3, N5, N6
N4
Louchadiere
E1
BL1, BL2
BL3
Kristjansson, 2003
Levi, 1990
Skalamælifell (this study)
Laschamp & previous studies at Skalamælifell
Laschamp
Olby
c)
CH89-9
JPC-14
MD94-103
MD95-2034
MD02-2551
MD02-2552
PS2644-5
d)

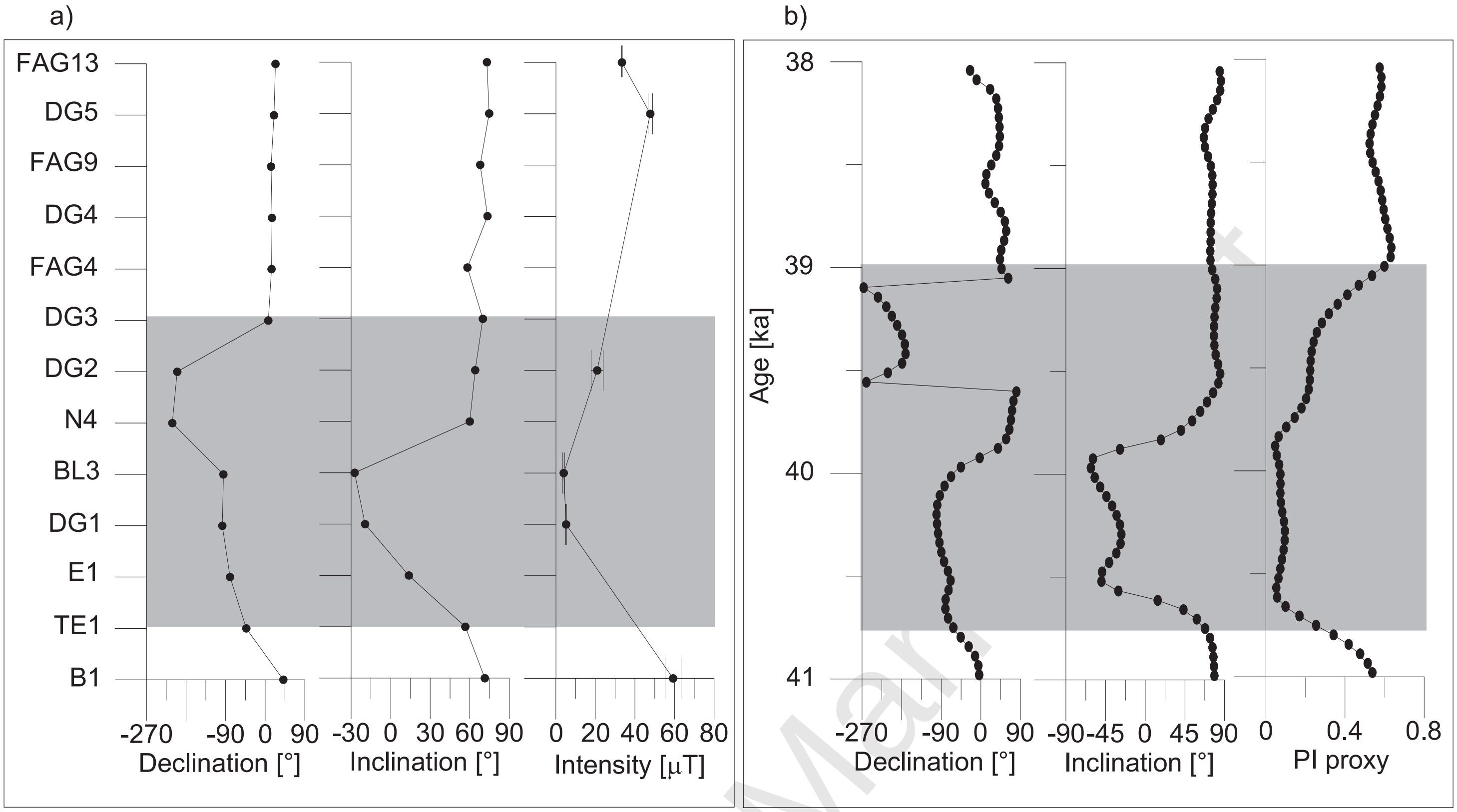
a)
FAG13
DG5
FAG9
DG4
FAG4
DG3
DG2
N4
BL3
DG1
E1
TE1
B1
-270 -90 0 90
Declination [°]
-30 0 30 60 90
Inclination [°]
0 20 40 60 80
Intensity [μT]
b)
38
39
40
41
Age [ka]
-270 -90 0 90
Declination [°]
-90-45 0 45 90
Inclination [°]
0 0.4 0.8
PI proxy

Table 1: Paleodirectional results.

Site	Long [°]	Lat [°]	n	N(N_{gc})	Dec [°]	Inc [°]	k	α_{95} [°]	VGP_{Long} [°]	VGP_{Lat} [°]
Excursion										
Bleikshóll										
BL1	-22.3367706	63.8650725	6	4 (1)	261.4	-20.2	249	6.2	250.7	-13.1
BL2	-22.3377301	63.8667618	6	6	263.3	-18.9	322	3.7	249.4	-11.7
BL3	-22.3373079	63.8670291	5	5	264.9	-27.3	143	6.4	245.7	-15.2
Einbúi										
E1	-22.3128764	63.8786999	6	6 (5)	280.1	13.8	70	9.6	241.7	10.7
Nátthagakriki										
N1	-22.2897031	63.8762336	6	6	158.5	64.9	112	6.4	353.4	22
N2	-22.2905105	63.8789943	6	5	162.6	65.8	164	6	350.2	22.8
N3	-22.2905105	63.8789943	6	6	154.8	64	304	3.8	356.3	21.4
N4	-22.2943194	63.8823834	6	6	148.8	60	1466	1.8	1.97	17.7
N5	-22.2943194	63.8823834	6	6	162.9	61.4	392	3.4	350.8	17.3
N6	-22.3039511	63.8854599	6	6	161.3	64.3	397	3.4	351.5	21
Tephra										
TE1	-22.3295086	63.8629993	6	4	317	56.6	110	8.8	222.4	53.1
Normal polarity										
Base										
B1	-22.3182179	63.8763219	12	10	41.3	71.4	583	2	69.4	68.4
Fagradalsfjall										
FAG1	-22.3141554	63.8829489	6	5	12.2	70.4	2104	1.7	118.5	78.8
FAG2	-22.3141554	63.8829489	4	4	4.7	71	93	9.6	139.9	81.2
FAG3	-22.3141554	63.8829489	5	4	3.2	68.1	109	8.9	148.6	77.2
FAG4	-22.3141554	63.8829489	6	6	14.5	58.2	499	3	131.7	63.6
FAG5	-22.3141554	63.8829489	3	3	12.2	76.1	140	10.5	64.5	84.6
FAG6	-22.3141554	63.8829489	6	5	4.7	72.2	188	5.6	136.3	83
FAG7	-22.3141554	63.8829489	5	5	19.7	71.3	325	4.3	97.7	77.4
FAG8	-22.3141554	63.8829489	4	4	26.5	74.9	803	3.2	66.1	77.8
FAG9	-22.3141554	63.8829489	6	6	13.4	67.9	339	3.6	122.7	75.2
FAG10	-22.3141554	63.8829489	3	3	35.3	72.6	80	13.9	70.7	72.1
FAG11	-22.3141554	63.8829489	6	5	11.7	75.1	146	6.3	82.1	84.4
FAG12	-22.3141554	63.8829489	5	5 (1)	14.7	75.1	293	4.6	76.9	83.1
FAG13	-22.3141554	63.8829489	6	6 (2)	23.5	73	219	4.7	82.2	77.6
Festarfjall										
FS1	-22.3341365	63.8578412	6	6	68.7	80.8	292	3.9	19.7	64.6
FS2	-22.3362097	63.8580434	6	6	86.1	75.7	154	5.4	28.8	54.4
Siglubergsháls										
SI1	-22.3289044	63.8610773	6	5	73.3	79.5	173	5.8	23.5	62.4
SI2	-22.3289044	63.8610773	6	6	64.6	77.1	233	4.4	35.1	63.5
Directional groups DG										
DG1: BL1,BL2			12	10 (1)	262.5	-19.4	328	2.7	250	-12.3
DG2: N1,N2,N3,N5,N6			30	29	160.0	64.1	218	1.8	352.5	20.8
DG3: FAG1,FAG2,FAG3			15	13	7	69.9	175	3.1	134.8	79.3
DG4: FAG5,FAG6,FAG7,FAG8			18	17	15.4	73.4	212	2.5	93.2	81.4
DG5: FAG10,FAG11,FAG12			14	13(1)	18.9	74.7	150	3.4	75.6	81.0
DG6: SI1,SI2,FS1			18	17	68.3	79.2	231	2.4	26.3	63.7

Site	Long [°]	Lat [°]	n	N(N_{gc})	Dec [°]	Inc [°]	k	α_{95} [°]	VGP_{Long} [°]	VGP_{Lat} [°]

Geographic coordinates were determined by GPS (WGS84). n corresponds to the amount of treated samples, N(N_{gc}) is the number of samples used for calculation of mean direction and in parenthesis those analyzed using great circle. Also shown are declination, inclination, k, α_{95} as well as virtual geomagnetic pole (VGP) coordinates.

Table 2: Paleointensity results

site	n/N	ID	T_{min}	T_{max}	N_p	f	g	q	w	F $\pm$ σ	$F_w \pm \sigma_w$	$F_a \pm \sigma_a$	
				[°C]	[°C]						[μT]	[μT]	[μT]
Excursion													
BL1	4/4	BL1-1D	20	430	8	0.35	0.73	3.5	1.4	5.8 $\pm$ 0.4	5.2 $\pm$ 0.2	5.2 $\pm$ 0.2	
		BL1-2E	100	490	9	0.34	0.81	3.8	1.4	5.1 $\pm$ 0.4			
		BL1-3E	20	430	8	0.31	0.59	2.7	1.1	5.1 $\pm$ 0.4			
		BL1-5C	200	460	7	0.35	0.59	2.4	1.1	4.6 $\pm$ 0.4			
BL2	0/3												
BL3	4/4	BL3-1D	390	550	6	0.76	0.68	12.3	6.1	4.0 $\pm$ 0.2	4.0 $\pm$ 0.4	4.0 $\pm$ 0.4	
		BL3-3E	20	610	14	0.88	0.79	7.5	2.2	3.9 $\pm$ 0.4			
		BL3-4D	250	490	7	0.58	0.76	8.4	3.8	5.0 $\pm$ 0.3			
		BL3-5D	300	570	10	0.71	0.72	6.8	2.4	2.8 $\pm$ 0.2			
N1	1/3	N1-5D	20	550	11	0.95	0.86	21.4	7.1	22.7 $\pm$ 0.9	22.7	19.9 $\pm$ 2.4	
N2	1/3	N2-1D	60	180	5	0.6	0.68	6.1	3.5	18.5 $\pm$ 1.2	18.5		
N5	0/2												
N6	4/4	N6-1D	120	420	11	0.39	0.78	5.4	1.8	18.5 $\pm$ 1.0	18.4 $\pm$ 0.4		
		N6-2D	270	570	11	0.95	0.80	49.5	16.5	18.3 $\pm$ 0.3			
		N6-3E	120	420	11	0.35	0.83	2.5	0.8	22.0 $\pm$ 2.5			
		N6-4D	120	420	11	0.44	0.87	7.9	2.6	18.0 $\pm$ 0.9			
Normal polarity													
B1	3/4	B1-1C	200	490	8	0.4	0.77	3.7	1.5	61.9 $\pm$ 5.2	59.3 $\pm$ 4.1	59.3 $\pm$ 4.1	
		B1-4D	300	520	7	0.4	0.78	4.7	2.1	65.3 $\pm$ 4.3			
		B1-5D	300	490	6	0.35	0.76	5.4	2.7	52.3 $\pm$ 2.6			
FAG7	0/2												
FAG8	0/3												
FAG11	4/4	FAG11-1C	20	350	6	0.37	0.79	3	1.5	47.6 $\pm$ 4.6	47.8 $\pm$ 1.1	47.8 $\pm$ 1.1	
		FAG11-4F	350	550	7	0.86	0.77	17.6	7.9	45.3 $\pm$ 1.7			
		FAG11-5E	250	550	9	0.85	0.82	15.3	5.8	49.8 $\pm$ 2.3			
		FAG11-6D	20	610	14	0.97	0.85	15.4	4.4	48.6 $\pm$ 2.6			
FAG12	0/3												
FAG13	2/3	FAG13-1B	190	430	9	0.36	0.81	2.5	1	32.7 $\pm$ 3.8	33.5 $\pm$ 0.2	33.5 $\pm$ 0.2	
		FAG13-6E	20	570	19	0.97	0.89	46.3	11.2	33.5 $\pm$ 0.6			
FS2	2/4	FS2-1D	20	570	19	0.98	0.89	33.4	8.1	27.0 $\pm$ 0.7	28.5 $\pm$ 2.2	28.5 $\pm$ 2.2	
		FS2-6D	60	240	7	0.57	0.78	15.2	6.8	31.7 $\pm$ 0.9			
SI1	0/3												
SI2	1/3	SI2-2D	60	570	18	0.94	0.86	79.3	19.8	27.4 $\pm$ 0.3	27.4	27.4	

n/N is the number of successful determinations per flow versus the number of measured specimens (ID), T_{min} to T_{max} gives the temperature range used for paleointensity calculation and N_p the number of independent and successive points in this interval. f, g, q, w represent the fraction of NRM, the gap factor, the quality factor (Coe et al., 1978) and the weighting factor (Prévot et al., 1985). F, σ are individual paleointensity and standard deviation, F_w and σ_w are weighted mean paleointensity and weighted standard deviation (using q) for each flow and F_a and σ_a are arithmetic mean paleointensity and standard deviation for the directional groups.